J. Plasma Phys. (2024), *vol*. 90, 905900121
Published by Cambridge University Press
doi:10.1017/S002237782400014X

Modulational instability of the interacting electron whistlers and magnetosonic perturbations

Jiao-Jiao Cheng[1],†, **Fang-Ping Wang**[1], **Zhong-Zheng Li**[2] and **Wen-Shan Duan**[1],†

[1]College of Physics and Electronic Engineering, Northwest Normal University, Lanzhou 730070, PR China

[2]Department of Physics, Gansu Normal University For Nationalities, Hezuo 747000, PR China

(Received 8 August 2023; revised 17 January 2024; accepted 17 January 2024)

A modulational instability of nonlinearly interacting electron whistlers and magnetosonic perturbations is studied in the present paper. For typical parameters, there is no modulational instability. However, modulational instability appears in special cases. For example, when the whistler wavenumber is small enough, there is modulational instability. Its growth rate decreases as the angle between the external magnetic field and the perturbed wave's direction increases, while it increases as the whistler wavenumber increases. It is also found that there is no modulational instability when the whistler wavenumber is larger than a critical value ($k_0 > 0.05$), in which the perturbed wave frequency increases as the angle between the external magnetic field and the perturbed wave's direction increases when the angle between the external magnetic field and the perturbed wave's direction is large enough. Whereas, the perturbed wave frequency first increases as the whistler wavenumber increases, reaches a peak value and then decreases as whistler wavenumber increases.

Keywords: plasma instabilities, plasma nonlinear phenomena, plasma waves

1. Introduction

Whistler waves are commonly observed phenomena in both space plasma and laboratory plasma (Stenzel 1999). They are a special type of electromagnetic wave found in various plasma environments, including atmospheric lightning, intense particle flows, magnetospheric turbulence, shock waves and even antennas in laboratory experiments. The formation of whistler waves involves multiple factors in plasma physics, such as electron beams, magnetic field instability and magnetic reconnection (Fujimoto & Sydora 2008; Choi *et al.* 2022). Non-thermal whistler waves are a unique type of electromagnetic wave propagating in plasmas, primarily along geomagnetic field lines, playing a crucial role in fast magnetic reconnection processes. Particularly in the presence of sheared magnetic fields, two-dimensional whistler waves demonstrate remarkable abilities, serving as a medium to facilitate fast magnetic reconnection (Li *et al.* 2014; Li, Wang &

† Email addresses for correspondence: chengjj3863@126.com, duanws@nwnu.edu.cn

Lu 2023), a fundamental process in rapidly rearranging magnetic field lines. This process is essential for the energization and acceleration of electrons in the plasma (Hoshino *et al.* 2001). Simultaneously, the energy released during magnetic reconnection may excite two-dimensional whistler waves, and the presence of these waves can, in turn, influence the dynamical evolution of magnetic reconnection (Bell *et al.* 2002; Horne *et al.* 2005). This interaction involves energy release, dynamical evolution and potential observation of nonlinear effects, contributing significantly to a deeper understanding of wave phenomena and magnetic field structure evolution in plasmas.

In plasma physics, whistler waves and magnetosonic perturbations play a crucial role in understanding the complex dynamics of space and laboratory plasmas. Extensive scholarly research has been dedicated to unravelling the intricate properties and behaviours of whistler waves. Notably, a recent laboratory experiment employed a non-stationary magnetic field (Kostrov *et al.* 2003; Gushchin *et al.* 2004), yielding significant insights into the self-focusing phenomenon exhibited by whistlers propagating parallel to the magnetic field direction (Karpman & Shagalov 1984; Karpman, Kaufman & Shagalov 1992; Eliasson & Shukla 2005*a*; Gupta, Choudhry & Bhardwaj 2023). This unique behaviour resulted in the formation of isolated wave packets (Gaster & Grant 1975). Experiments also have revealed the capture of whistlers within ducts characterized by depleted plasma density, highlighting the interplay between wave propagation and plasma density variations (Nassiri 2008; Singh 2013). Moreover, the confinement of whistlers within magnetic tubes, characterized by localized regions of enhanced magnetic fields in a uniform plasma density environment, has been experimentally demonstrated (Gushchin *et al.* 2005). Additionally, the generation of electrostatic ion cyclotron waves has been observed in large-volume spiral reactors, indicative of the parametric instability associated with high-amplitude whistlers (Sutherland, Giles & Boswell 2005; Tripathi & Kumara 2008). Findings from the Freja satellite (Huang, Wang & Song 2004) also reveal the occurrence of envelope whistler solitary waves accompanied by plasma density cavities.

Modulational instability refers to the phenomenon in nonlinear systems where, due to the interaction between nonlinear effects and dispersion effects, plane waves undergo filamentation under high-intensity conditions. This results in small-amplitude perturbations experiencing exponential growth, ultimately leading to the modulation or formation of spatial structures in the wave (Inan 1987; Meier *et al.* 2004; Shukla *et al.* 2005). Modulational instability is widely observed in various fields of physics, including fluid dynamics, nonlinear optics and plasma physics. Therefore, investigating the development of modulational instability and its propagation in plasmas holds significant importance (Gurovich & Karpman 1969; Tai, Hasegawa & Tomita 1986; Kivshar 1992). Considering the mass potential of spatiotemporal correlation in whistler waves (Tskhakaya 1981; Zhu *et al.* 2023), the modulational instability of nonlinearly interacting electron whistlers and magnetosonic perturbations is studied in the present paper (Karpman *et al.* 1995; Das *et al.* 2002). It is found that, for typical plasma parameters, there is no modulational instability. However, modulational instability appears in special cases. It is shown that when the whistler wavenumber is small enough, there is modulational instability. It is also found that there is no modulational instability when the whistler wavenumber is larger than a critical value.

The content of the paper is organized as follows. In § 2, the coupled nonlinear equations which describe the dynamics of the whistler envelope in the presence of the slowly varying magnetic field have been presented. Section 3 obtains solutions for background and perturbation waves. Section 4 discusses various special cases. Section 5 establishes

https://doi.org/10.1017/S002237782400014X Published online by Cambridge University Press

the instability conditions for perturbation waves and § 6 provides a summary and conclusions.

2. Theoretical model

We start by obtaining the relevant equations for nonlinearly coupled whistlers and magnetosonic perturbations in a fully ionized electron–ion plasma. The fundamental equations for the plasma slow response concerning magnetosonic disturbances can be expressed as follows (Eliasson & Shukla 2005*b*):

$$\frac{\partial n_1}{\partial t} + n_0 \nabla \cdot \boldsymbol{v_1} = 0, \tag{2.1}$$

$$\frac{\partial \boldsymbol{v_1}}{\partial t} = -\frac{C_s^2 \nabla n_1}{n_0} - \frac{1}{4\pi m_i n_0} \boldsymbol{B_0} \times (\nabla \times \boldsymbol{B_1}) + \frac{\boldsymbol{F}}{m_i}, \tag{2.2}$$

$$\frac{\partial \boldsymbol{B_1}}{\partial t} - \nabla \times (\boldsymbol{v_1} \times \boldsymbol{B_0}) = 0. \tag{2.3}$$

The total quantities for ion density, ion fluid velocity and magnetic field can be expressed as follows: $n = n_0 + n_1$, $\boldsymbol{B} = \boldsymbol{B}_0 + \boldsymbol{B}_1$; where n is the total electron number density, n_1 is the electron density perturbation, $\boldsymbol{B}$ is the total magnetic field vector, $\boldsymbol{B_1}$ is the magnetic field perturbation, $\boldsymbol{v_1}$ is the velocity, n_0 denotes the electron number density in the absence of any perturbations, $\boldsymbol{B_0} = B_0 \hat{\boldsymbol{z}}$ represents the uniform magnetic field in the direction of z, where $\hat{\boldsymbol{z}}$ is a unit vector along the z axis, C_s is the speed of ion acoustic waves, m_i is the mass of ions.

The ponderomotive force associated with whistler waves can be expressed as follows:

$$\boldsymbol{F} = \hat{\boldsymbol{z}} \epsilon \left(\frac{\partial}{\partial z} + \frac{2}{V_g} \frac{\partial}{\partial t} \right) \frac{|E|^2}{8\pi n_0} - \frac{\epsilon \alpha}{1-\alpha} \nabla_\perp \frac{|E|^2}{8\pi n_0}, \tag{2.4}$$

the differentiation operator in this context is defined as $\nabla_\perp = \hat{\boldsymbol{x}} \partial/\partial x + \hat{\boldsymbol{y}} \partial/\partial y$, where $\hat{\boldsymbol{x}}$ and $\hat{\boldsymbol{y}}$ are unit vectors along the x and y directions, respectively. Additionally, the following parameters are defined: $\epsilon = \omega_{\rm pe}^2/\omega_0(\omega_{\rm ce} - \omega_0)$ and $\alpha = \omega_0/\omega_{\rm ce}$; where $\omega_{\rm pe}$ is the electron plasma frequency, $\omega_{\rm ce}$ is the electron cyclotron frequency and ω_0 is the whistler waves frequency. The frequency of whistler waves with wavenumber k_0 is given by $\omega_0 = c^2 k_0^2 \omega_{\rm ce}/(\omega_{\rm pe}^2 + c^2 k_0^2)$, where c is the speed of light in a vacuum.

These equations can be further simplified to study the behaviour of nonlinearly coupled whistlers and magnetosonic perturbations in an electron–ion plasma. By eliminating the perpendicular components of the magnetic field, B_{1x} and B_{1y}, and velocity, v_{1x} and v_{1y}, the system of equations (2.1)–(2.3) can be given by

$$\frac{\partial^2 b}{\partial t^2} = C_s^2 \nabla_\perp^2 N + C_A^2 \left(\nabla_\perp^2 + \frac{\partial^2}{\partial z^2} \right) b + \frac{\epsilon \alpha}{1-\alpha} \nabla_\perp^2 \frac{|E|^2}{8\pi m_i n_0}, \tag{2.5}$$

$$\frac{\partial}{\partial t}(N - b) = -\frac{\partial v_{1z}}{\partial z}, \tag{2.6}$$

$$\frac{\partial v_{1z}}{\partial t} = -C_s^2 \frac{\partial N}{\partial z} + \epsilon \left(\frac{\partial}{\partial z} + \frac{2}{V_g} \frac{\partial}{\partial t} \right) \frac{|E|^2}{8\pi m_i n_0}, \tag{2.7}$$

where $C_A = B_0/(4\pi m_i n_0)^{1/2}$ is the Alfvén speed; and we have denoted $b = B_{1z}/B_0$ and $N = n_1/n_0$.

https://doi.org/10.1017/S002237782400014X Published online by Cambridge University Press

We now focus on the modulated whistlers with right-hand circular polarization and assume that $\boldsymbol{E} = (1/2)E(x, y, z, t)(\hat{\boldsymbol{x}} + \mathrm{i}\hat{\boldsymbol{y}}) \exp[\mathrm{i}(k_0 z - \omega_0 t)] + c.c.$, where E represents the slowly varying envelope of the whistler electric field and $c.c.$ denotes the complex conjugate. The equation governing the whistler field envelope is given by (Shukla & Stenflo 1995)

$$\mathrm{i}\left(\frac{\partial E}{\partial t} + V_g \frac{\partial E}{\partial z}\right) + \frac{V_g'}{2}\frac{\partial^2 E}{\partial z^2} + \frac{T}{2}\nabla_\perp^2 E + \{\omega_0[(1-\alpha)N - b] - k_0 v_{1z}\}E = 0, \tag{2.8}$$

where $V_g = 2(1-\alpha)\omega_0/k_0$ is the group velocity, $V_g' = 2(1-\alpha)(1-4\alpha)\omega_0/k_0^2$ and $T = (1-2\alpha)\omega_0/k_0^2$ are the group dispersion coefficients. Notice that V_g, V_g' and T can change sign depending on the ratio α, which is critical for the formation of localized nonlinear wave packets at different frequencies. The $k_0 v_{1z}$ term represents the Doppler shift due to the plasma streaming along the magnetic field.

In the special case where the wave packet is modulated along the z axis and moving at a speed close to the group velocity V_g, we can make certain assumptions to simplify the equations. Assuming $b = 0$ and N depends only on $\xi = z - V_g t$, we can integrate (2.6) to obtain $v_{1z} = NV_g$, and subsequently, $k_0 v_{1z} = 2\omega_0(1-\alpha)N$.

Assuming that N, b, v_{1z} and $|E|$ are functions of the variables $(\xi, \boldsymbol{x}_\perp, \tau)$, where $\tau = t$ and that $\partial/\partial\tau << \partial/\partial\xi$, (2.6)–(2.8) can be rewritten as follows:

$$V_g^2 \frac{\partial^2 b}{\partial \xi^2} = C_s^2 \nabla_\perp^2 N + C_A^2\left(\nabla_\perp^2 + \frac{\partial^2}{\partial \xi^2}\right) b + \frac{\epsilon\alpha}{1-\alpha}\nabla_\perp^2 \frac{|E|^2}{8\pi m_i n_0}, \tag{2.9}$$

$$-V_g \frac{\partial}{\partial \xi}(N - b) = -\frac{\partial v_{1z}}{\partial \xi}, \tag{2.10}$$

$$-V_g \frac{\partial v_{1z}}{\partial \xi} = -C_s^2 \frac{\partial N}{\partial \xi} - \epsilon \frac{\partial}{\partial \xi}\frac{|E|^2}{8\pi m_i n_0}. \tag{2.11}$$

By integrating (2.10) and (2.11), we have $V_g(N - b) = v_{1z}$ and $V_g v_{1z} = C_s^2 N + \epsilon|E|^2/8\pi m_i n_0$, then, (2.9) becomes

$$\frac{\partial^2 b}{\partial \xi^2} - \nu^2 \nabla_\perp^2 b = Q\epsilon\nabla_\perp^2 \frac{|E|^2}{8\pi m_i n_0}, \tag{2.12}$$

where $\nu^2 = [C_s^2 V_g^2/(V_g^2 - C_s^2) + C_A^2]/(V_g^2 - C_A^2)$ and $Q = [C_s^2/(V_g^2 - C_s^2) + \alpha/(1-\alpha)]/(V_g^2 - C_A^2)$. Furthermore, (2.8) becomes

$$\mathrm{i}\frac{\partial E}{\partial \tau} + \frac{V_g'}{2}\frac{\partial^2 E}{\partial \xi^2} + \frac{T}{2}\nabla_\perp^2 E - \frac{\omega_0}{V_g^2 - C_s^2}\left\{[\alpha V_g^2 + (1-2\alpha)C_s^2]b + (1-\alpha)\epsilon\frac{|E|^2}{8\pi m_i n_0}\right\}E = 0. \tag{2.13}$$

Equations (2.12) and (2.13) are the coupled nonlinear equations which describes the dynamics of the whistler envelope in the presence of the slowly varying magnetic field.

3. Instability of the whistler envelope waves

3.1. *Linear background wave*

To understand the linear background wave, we make the assumptions $E = a_0 \exp(\mathrm{i}\theta_0(\tau))$, $G = d_0 \exp(\mathrm{i}\beta_0(\tau))$, $b = |G|^2$, where a_0 and d_0 are constants. Consequently, we obtain $|E|^2 = a_0^2$, $b = d_0^2$, $\nabla_\perp^2 b = 0$. Additionally, we have $\nabla_\perp^2 E = 0$, $\partial^2 b/\partial\xi^2 = 0$,

https://doi.org/10.1017/S002237782400014X Published online by Cambridge University Press

$\partial^2 E/\partial\xi^2 = 0$, $\partial E/\partial\tau = \mathrm{i}E\partial\theta_0/\partial\tau$, $\partial^2 E/\partial\tau^2 = -E(\partial\theta_0/\partial\tau)^2 + \mathrm{i}E\partial^2\theta_0/\partial\tau^2$. After substituting these equations into (2.12) and (2.13), we have

$$\theta_0(\tau) = -\frac{\omega_0\tau}{V_g^2 - C_s^2}\left\{[\alpha V_g^2 + (1-2\alpha)C_s^2]d_0^2 + (1-\alpha)\epsilon\frac{a_0^2}{8\pi m_i n_0}\right\}. \tag{3.1}$$

Then, we have

$$E = a_0\exp\left(-\mathrm{i}\frac{\omega_0}{V_g^2 - C_s^2}\left\{[\alpha V_g^2 + (1-2\alpha)C_s^2]d_0^2 + (1-\alpha)\epsilon\frac{c_0^2}{8\pi m_i n_0}\right\}\tau\right), \tag{3.2}$$

$$b = d_0^2. \tag{3.3}$$

Equations (3.2) and (3.3) represent the linear background wave. Its frequency is

$$\omega_{bc} = \frac{\omega_0}{V_g^2 - C_s^2}\left\{[\alpha V_g^2 + (1-2\alpha)C_s^2]d_0^2 + (1-\alpha)\epsilon\frac{a_0^2}{8\pi m_i n_0}\right\}. \tag{3.4}$$

3.2. *Nonlinear wave*

For more general case of the nonlinear wave, we assume

$$E(x, y, \xi, \tau) = a(x, y, \xi, \tau)\exp[\mathrm{i}\theta(x, y, \xi, \tau)], \tag{3.5}$$

$$G(x, y, \xi, \tau) = d(x, y, \xi, \tau)\exp[\mathrm{i}\beta(x, y, \xi, \tau)], \tag{3.6}$$

$$b(x, y, \xi, \tau) = |G(x, y, \xi, \tau)|^2. \tag{3.7}$$

Then we have $|E|^2 = |a(x, y, \xi, \tau)|^2$, $b = |d(x, y, \xi, \tau)|^2$, and the following equations:

$$\frac{\partial^2|d|^2}{\partial\xi^2} - \nu^2\left(\frac{\partial^2|d|^2}{\partial x^2} + \frac{\partial^2|d|^2}{\partial y^2}\right) = Q\epsilon\frac{\dfrac{\partial^2|a|^2}{\partial x^2} + \dfrac{\partial^2|a|^2}{\partial y^2}}{8\pi m_i n_0}, \tag{3.8}$$

$$\begin{aligned}
&\mathrm{i}\left(\frac{\partial a}{\partial\tau} + \mathrm{i}a\frac{\partial\theta}{\partial\tau}\right) + \frac{V_g'}{2}\left[\frac{\partial^2 a}{\partial\xi^2} + 2\mathrm{i}\frac{\partial a}{\partial\xi}\frac{\partial\theta}{\partial\xi} - a\left(\frac{\partial\theta}{\partial\xi}\right)^2 + \mathrm{i}a\frac{\partial^2\theta}{\partial\xi^2}\right] + \frac{T}{2}\left\{\frac{\partial^2 a}{\partial x^2} + \frac{\partial^2 a}{\partial y^2}\right.\\
&\quad\left.+2\mathrm{i}\left(\frac{\partial a}{\partial x}\frac{\partial\theta}{\partial x} + \frac{\partial a}{\partial y}\frac{\partial\theta}{\partial y}\right) - a\left[\left(\frac{\partial\theta}{\partial x}\right)^2 + \left(\frac{\partial\theta}{\partial y}\right)^2\right] + \mathrm{i}a\left(\frac{\partial^2\theta}{\partial x^2} + \frac{\partial^2\theta}{\partial y^2}\right)\right\}\\
&\quad - \frac{a\omega_0}{V_g^2 - C_s^2}\left\{[\alpha V_g^2 + (1-2\alpha)C_s^2]|d|^2 + (1-\alpha)\epsilon\frac{|a|^2}{8\pi m_i n_0}\right\} = 0.
\end{aligned} \tag{3.9}$$

We obtain two equations from both real and imaginary terms of (3.9) as follows:

$$\begin{aligned}
&-a\frac{\partial\theta}{\partial\tau} + \frac{V_g'}{2}\frac{\partial^2 a}{\partial\xi^2} - \frac{aV_g'^2}{2}\left(\frac{\partial\theta}{\partial\xi}\right)^2 + \frac{T}{2}\frac{\partial^2 a}{\partial x^2} + \frac{T}{2}\frac{\partial^2 a}{\partial y^2} - \frac{aT}{2}\left(\frac{\partial\theta}{\partial x}\right)^2\\
&\quad - \frac{aT}{2}\left(\frac{\partial\theta}{\partial y}\right)^2 - \frac{a\omega_0}{V_g^2 - C_s^2}\left\{[\alpha V_g^2 + (1-2\alpha)C_s^2]|d|^2 + (1-\alpha)\epsilon\frac{|a|^2}{8\pi m_i n_0}\right\} = 0,
\end{aligned} \tag{3.10}$$

https://doi.org/10.1017/S002237782400014X Published online by Cambridge University Press

$$\frac{\partial a}{\partial \tau}+V_g'\frac{\partial a}{\partial \xi}\frac{\partial \theta}{\partial \xi}+\frac{aV_g'}{2}\frac{\partial^2\theta}{\partial \xi^2}+T\frac{\partial a}{\partial x}\frac{\partial \theta}{\partial x}+T\frac{\partial a}{\partial y}\frac{\partial \theta}{\partial y}+\frac{aT}{2}\frac{\partial^2\theta}{\partial x^2}+\frac{aT}{2}\frac{\partial^2\theta}{\partial y^2}=0. \tag{3.11}$$

We rewrote (3.8) as follows:

$$\frac{\partial^2|d|^2}{\partial \xi^2}-\nu^2\left(\frac{\partial^2|d|^2}{\partial x^2}+\frac{\partial^2|d|^2}{\partial y^2}\right)=Q\epsilon\frac{\dfrac{\partial^2|a|^2}{\partial x^2}+\dfrac{\partial^2|a|^2}{\partial y^2}}{8\pi m_i n_0}. \tag{3.12}$$

Further, we assume that

$$a(x,y,\xi,\tau)=a_0(\tau)+\varepsilon a_1(x,y,\xi,\tau), \tag{3.13}$$

$$d(x,y,\xi,\tau)=d_0(\tau)+\varepsilon d_1(x,y,\xi,\tau), \tag{3.14}$$

$$\theta(x,y,\xi,\tau)=\theta_0(\tau)+\varepsilon\theta_1(x,y,\xi,\tau), \tag{3.15}$$

where all the variables are complex, as later indicated by their complex conjugates.

Then (3.10)–(3.12) become

$$\begin{aligned}&(a_0+\varepsilon a_1)\left(\frac{\partial\theta_0}{\partial\tau}+\varepsilon\frac{\partial\theta_1}{\partial\tau}\right)+\frac{\varepsilon^2V_g'}{2}(a_0+\varepsilon a_1)\left(\frac{\partial\theta_1}{\partial\xi}\right)^2+\frac{\varepsilon^2T}{2}(a_0+\varepsilon a_1)\left(\frac{\partial\theta_1}{\partial x}\right)^2\\&+\frac{\varepsilon^2T}{2}(a_0+\varepsilon a_1)\left(\frac{\partial\theta_1}{\partial y}\right)^2-\frac{\varepsilon V_g'}{2}\frac{\partial^2a_1}{\partial\xi^2}-\frac{\varepsilon T}{2}\frac{\partial^2a_1}{\partial x^2}-\frac{\varepsilon T}{2}\frac{\partial^2a_1}{\partial y^2}\\&+\frac{\omega_0}{V_g^2-C_s^2}(a_0+\varepsilon a_1)[\alpha V_g^2+(1-2\alpha)C_s^2][|d_0|^2+\varepsilon(d_0d_1^*+d_1d_0^*)+\varepsilon^2|d_1|^2]\\&+\frac{\omega_0}{V_g^2-C_s^2}(a_0+\varepsilon a_1)(1-\alpha)\epsilon\frac{1}{8\pi m_in_0}[|a_0|^2+\varepsilon(a_0a_1^*+a_1a_0^*)\varepsilon^2|a_1|^2]=0,\end{aligned} \tag{3.16}$$

$$\begin{aligned}&\frac{a_0}{\partial\tau}+\varepsilon\frac{\partial a_1}{\partial\tau}+\varepsilon^2V_g'\frac{\partial a_1}{\partial\xi}\frac{\partial\theta_1}{\partial\xi}+\varepsilon\frac{a_0V_g'}{2}\frac{\partial^2\theta_1}{\partial\xi^2}+\varepsilon^2\frac{a_1V_g'}{2}\frac{\partial^2\theta_1}{\partial\xi^2}+\varepsilon^2T\frac{\partial a_1}{\partial x}\frac{\partial\theta_1}{\partial x}\\&+\varepsilon^2T\frac{\partial a_1}{\partial y}\frac{\partial\theta_1}{\partial y}+\varepsilon\frac{a_0T}{2}\frac{\partial^2\theta_1}{\partial x^2}+\varepsilon^2\frac{a_1T}{2}\frac{\partial^2\theta_1}{\partial x^2}+\varepsilon\frac{a_0T}{2}\frac{\partial^2\theta_1}{\partial y^2}+\varepsilon^2\frac{a_1T}{2}\frac{\partial^2\theta_1}{\partial y^2}=0,\end{aligned} \tag{3.17}$$

$$\begin{aligned}&\varepsilon d_0\frac{\partial^2d_1^*}{\partial\xi^2}+\varepsilon d_0^*\frac{\partial^2d_1}{\partial\xi^2}+\varepsilon^2\frac{\partial^2|d_1|^2}{\partial\xi^2}-\varepsilon\nu^2d_0\frac{\partial^2d_1^*}{\partial x^2}-\varepsilon\nu^2d_0^*\frac{\partial^2d_1}{\partial x^2}-\varepsilon^2\nu^2\frac{\partial^2|d_1|^2}{\partial x^2}\\&-\varepsilon\nu^2d_0\frac{\partial^2d_1^*}{\partial y^2}-\varepsilon\nu^2d_0^*\frac{\partial^2d_1}{\partial y^2}-\varepsilon^2\nu^2\frac{\partial^2|d_1|^2}{\partial y^2}-\varepsilon\frac{Qa_0\epsilon}{8\pi m_in_0}\frac{\partial^2a_1^*}{\partial x^2}-\varepsilon\frac{Qa_0^*\epsilon}{8\pi m_in_0}\frac{\partial^2a_1}{\partial x^2}\\&-\varepsilon^2\frac{Q\epsilon}{8\pi m_in_0}\frac{\partial^2|a_1|^2}{\partial x^2}-\varepsilon\frac{Qa_0\epsilon}{8\pi m_in_0}\frac{\partial^2a_1^*}{\partial y^2}-\varepsilon\frac{Qa_0^*\epsilon}{8\pi m_in_0}\frac{\partial^2a_1}{\partial y^2}-\varepsilon^2\frac{Q\epsilon}{8\pi m_in_0}\frac{\partial^2|a_1|^2}{\partial y^2}=0.\end{aligned} \tag{3.18}$$

The solutions for the lowest order ε^0 of (3.16)–(3.18) are as follows:

$$\theta_0(\tau)=-\left[\frac{\omega_0\alpha V_g^2|d_0|^2}{V_g^2-C_s}+\frac{\omega_0(1-2\alpha)C_s^2|d_0|^2}{V_g^2-C_s^2}+\frac{\epsilon\omega_0(1-\alpha)|a_0|^2}{8\pi m_in_)(V_g^2-C_s^20)}\right]\tau, \tag{3.19}$$

$$a_0(\tau)=E_{00}, \tag{3.20}$$

where E_{00} is any arbitrary constant and we assumed that $a_0=1$ in the numerical simulations.

https://doi.org/10.1017/S002237782400014X Published online by Cambridge University Press

We have the following equations at the next lowest order of ε^1:

$$
\begin{aligned}
&a_0\frac{\partial\theta_1}{\partial\tau}+a_1\frac{\partial\theta_0}{\partial\tau}-\frac{V_g'}{2}\frac{\partial^2 a_1}{\partial\xi^2}-\frac{T}{2}\frac{\partial^2 a_1}{\partial x^2}-\frac{T}{2}\frac{\partial^2 a_1}{\partial y^2}+\frac{a_0\omega_0\alpha V_g^2 d_0 d_1^*}{V_g^2-C_s^2}\\
&+\frac{a_0\omega_0\alpha V_g^2 d_1 d_0^*}{V_g^2-C_s^2}+\frac{a_1\omega_0\alpha V_g^2|d_0|^2}{V_g^2-C_s^2}+\frac{a_0\omega_0 C_s^2 d_0 d_1^*}{V_g^2-C_s^2}+\frac{a_0\omega_0 C_s^2 d_1 d_0^*}{V_g^2-C_s^2}\\
&+\frac{a_1\omega_0 C_s^2|d_0|^2}{V_g^2-C_s^2}-\frac{2a_0\alpha\omega_0 C_s^2 d_0 d_1^*}{V_g^2-C_s^2}-\frac{2a_0\alpha\omega_0 C_s^2 d_1 d_0^*}{V_g^2-C_s^2}-\frac{2a_1\alpha\omega_0 C_s^2|d_0|^2}{V_g^2-C_s^2}\\
&+\frac{\epsilon\omega_0 a_0^2 a_1^*}{V_g^2-C_s^2}\frac{1}{8\pi m_i n_0}+\frac{\epsilon|a_0|^2\omega_0 a_1}{V_g^2-C_s^2}\frac{1}{8\pi m_i n_0}+\frac{\epsilon a_1\omega_0|a_0|^2}{V_g^2-C_s^2}\frac{1}{8\pi m_i n_0}\\
&-\frac{\alpha\omega_0\epsilon a_0^2 a_1^*}{V_g^2-C_s^2}\frac{1}{8\pi m_i n_0}-\frac{|a_0|^2\alpha\omega_0\epsilon a_1}{V_g^2-C_s^2}\frac{1}{8\pi m_i n_0}-\frac{\epsilon a_1\alpha\omega_0|a_0|^2}{V_g^2-C_s^2}\frac{1}{8\pi m_i n_0}=0, \qquad (3.21)
\end{aligned}
$$

$$
\frac{\partial a_1}{\partial\tau}+\frac{a_0 V_g'}{2}\frac{\partial^2\theta_1}{\partial\xi^2}+\frac{a_0 T}{2}\frac{\partial^2\theta_1}{\partial x^2}+\frac{a_0 T}{2}\frac{\partial^2\theta_1}{\partial y^2}=0, \qquad (3.22)
$$

$$
\begin{aligned}
&d_0\frac{\partial^2 d_1^*}{\partial\xi^2}+d_0^*\frac{\partial^2 d_1}{\partial\xi^2}-\nu^2 d_0\frac{\partial^2 d_1^*}{\partial x^2}-\nu^2 d_0^*\frac{\partial^2 d_1}{\partial x^2}-\nu^2 d_0\frac{\partial^2 d_1^*}{\partial y^2}-\nu^2 d_0^*\frac{\partial^2 d_1}{\partial y^2}\\
&-\frac{Q a_0\epsilon}{8\pi m_i n_0}\frac{\partial^2 a_1^*}{\partial x^2}-\frac{Q a_0^*\epsilon}{8\pi m_i n_0}\frac{\partial^2 a_1}{\partial x^2}-\frac{Q a_0\epsilon}{8\pi m_i n_0}\frac{\partial^2 a_1^*}{\partial y^2}-\frac{Q a_0^*\epsilon}{8\pi m_i n_0}\frac{\partial^2 a_1}{\partial y^2}=0. \qquad (3.23)
\end{aligned}
$$

We now assume that the perturbations have a sinusoidal waveform with wavenumber $k=(k_x,k_y,k_\xi)$ and frequency ω as follows:

$$a_1 = A\exp(\mathrm{i}(k_x x+k_y y+k_\xi\xi-\omega\tau))+A^*\exp(-\mathrm{i}(k_x x+k_y y+k_\xi\xi-\omega\tau)), \qquad (3.24)$$

$$d_1 = D\exp(\mathrm{i}(k_x x+k_y y+k_\xi\xi-\omega\tau))+D^*\exp(-\mathrm{i}(k_x x+k_y y+k_\xi\xi-\omega\tau)), \qquad (3.25)$$

$$\theta_1 = \Theta\exp(\mathrm{i}(k_x x+k_y y+k_\xi\xi-\omega\tau))+\Theta^*\exp(-\mathrm{i}(k_x x+k_y y+k_\xi\xi-\omega\tau)). \qquad (3.26)$$

Substituting these equations into (3.21)–(3.23) we have

$$
\begin{aligned}
&\frac{\partial\theta_0}{\partial\tau}(A\mathrm{e}^{\mathrm{i}\chi}+A^*\mathrm{e}^{-\mathrm{i}\chi})+\left(\frac{k_x^2 T}{2}+\frac{k_y^2 T}{2}+\frac{k_\xi^2 V_g'}{2}\right)(A\mathrm{e}^{\mathrm{i}\chi}+A^*\mathrm{e}^{-\mathrm{i}\chi})\\
&+\frac{\omega_0\alpha V_g^2 d_0^2}{V_g^2-C_s^2}(C\mathrm{e}^{\mathrm{i}\chi}+C^*\mathrm{e}^{-\mathrm{i}\chi})+\frac{\omega_0 C_s^2 d_0^2(1-2\alpha)}{V_g^2-C_s^2}(C\mathrm{e}^{\mathrm{i}\chi}+C^*\mathrm{e}^{-\mathrm{i}\chi})\\
&+\frac{3\epsilon\omega_0 a_0^2(1-\alpha)}{8\pi m_i n_0(V_g^2-C_s^2)}(C\mathrm{e}^{\mathrm{i}\chi}+C^*\mathrm{e}^{-\mathrm{i}\chi})+\frac{2a_0\omega_0 C_s^2 d_0(1-2\alpha)}{V_g^2-C_s^2}(D\mathrm{e}^{\mathrm{i}\chi}+D^*\mathrm{e}^{-\mathrm{i}\chi})\\
&+\frac{2\alpha\omega_0 a_0 V_g^2 d_0}{V_g^2-C_s^2}(D\mathrm{e}^{\mathrm{i}\chi}+D^*\mathrm{e}^{-\mathrm{i}\chi})+\mathrm{i}\omega a_0(\Theta^*\mathrm{e}^{-\mathrm{i}\chi}-\Theta\mathrm{e}^{\mathrm{i}\chi})=0, \qquad (3.27)
\end{aligned}
$$

https://doi.org/10.1017/S002237782400014X Published online by Cambridge University Press

$$\mathrm{i}\omega(A^*\mathrm{e}^{-\mathrm{i}\chi} - A\mathrm{e}^{\mathrm{i}\chi}) - \left(\frac{a_0k_\xi^2V_g'}{2} + \frac{a_0k_x^2T}{2} + \frac{a_0k_y^2T}{2}\right)(\Theta\mathrm{e}^{\mathrm{i}\chi} + \Theta^*\mathrm{e}^{-\mathrm{i}\chi}) = 0, \tag{3.28}$$

$$\left(\frac{Qa_0\epsilon k_x^2}{8\pi m_in_0} + \frac{Qa_0\epsilon k_y^2}{8\pi m_in_0}\right)(A\,\mathrm{e}^{\mathrm{i}\chi} + A^*\mathrm{e}^{-\mathrm{i}\chi}) + (\nu^2d_0k_x^2 + \nu^2d_0k_y^2 - d_0k_\xi^2)(De^{\mathrm{i}\chi} + D^*\mathrm{e}^{-\mathrm{i}\chi}) = 0, \tag{3.29}$$

where $\chi = k_xx + k_yy + k_\xi\xi - \omega\tau$.

We have the following equations from the coefficient of the term of $\mathrm{e}^{\mathrm{i}\chi}$:

$$\left(\frac{k_x^2T}{2} + \frac{k_y^2T}{2} + \frac{k_\xi^2V_g'}{2} + \frac{2\epsilon\omega_0a_0^2(1-\alpha)}{8\pi m_in_0(V_g^2 - C_s^2)}\right)A + \left[\frac{2a_0\omega_0\alpha V_g^2d_0}{V_g^2 - C_s^2} + \frac{2a_0\omega_0C_s^2d_0(1-2\alpha)}{V_g^2 - C_s^2}\right]D - \mathrm{i}\omega a_0\Theta = 0, \tag{3.30}$$

$$\mathrm{i}\omega A + \left(\frac{a_0k_x^2T}{2} + \frac{a_0k_y^2T}{2} + \frac{a_0k_\xi^2V_g'}{2}\right)\Theta = 0, \tag{3.31}$$

$$\frac{Qa_0\epsilon(k_x^2 + k_y^2)}{8\pi m_in_0}A + (\nu^2d_0k_x^2 + \nu^2d_0k_y^2 - d_0k_\xi^2)D = 0. \tag{3.32}$$

In order to obtain the non-trivial solution from (3.30)–(3.32), we have the following equation:

$$\omega^2 = \left[\frac{1}{4}(k_x^2T + k_y^2T + k_\xi^2V_g') + \frac{\epsilon\omega_0a_0^2(1-\alpha)}{8\pi m_in_0(V_g^2 - C_s^2)} - \frac{\omega_0a_0^2Q\epsilon(\alpha V_g^2 + C_s^2 - 2\alpha C_s^2)}{8\pi m_in_0(V_g^2 - C_s^2)}\frac{k_x^2 + k_y^2}{k_\xi - \nu^2k_x^2 - \nu^2k_y^2}\right](k_x^2T + k_y^2T + k_\xi V_g'), \tag{3.33}$$

where $\omega_0 = c^2k_0^2\omega_{\mathrm{ce}}/(\omega_{\mathrm{pe}}^2 + c^2k_0^2)$, $\epsilon = \omega_{\mathrm{pe}}^2/\omega_0(\omega_{\mathrm{ce}} - \omega_0)$, $k_0 = \lambda_e^{-1}\alpha^{1/2}(1-\alpha)^{-1/2}$, $V_g = 2(1-\alpha)\omega_0/k_0$, $V_g' = 2(1-\alpha)(1-4\alpha)\omega_0/k_0^2$, $T = (1-2\alpha)\omega_0/k_0^2$, $\lambda_e = c/\omega_{\mathrm{pe}}$, $\alpha = \omega_0/\omega_{\mathrm{ce}}$, $\omega_{\mathrm{pe}} = (4\pi n_ee^2/m_e)^{1/2}$, $\omega_{\mathrm{ce}} = eB_0/m_e$, $C_s = (\gamma kT_i/m_i)^{1/2}$, $C_A = B_0/(4\pi m_in_e)^{1/2}$, $\nu^2 = [C_s^2V_g^2/(V_g^2 - C_s^2) + C_A^2]/(V_g^2 - C_A^2)$, $Q = [C_s^2/(V_g^2 - C_s^2) + \alpha/(1-\alpha)]/(V_g^2 - C_A^2)$.

Equation (3.33) is the dispersion relation of the perturbed wave.

4. Discussion for some special cases

To study the dispersion relation of the perturbed wave of (3.33), we consider three typical cases.

First, $(k_x, k_y, k_\xi) = (0, 0, k_\xi)$, in which the wave propagates in the direction of $\xi = z - V_gt$, i.e. in the z direction. In other words, the perturbed wave propagates in the direction of the external magnetic field. For this case, (3.33) becomes

$$\omega^2 = \left[\frac{1}{4}k_\xi^2V_g' + \frac{\epsilon\omega_0a_0^2(1-\alpha)}{8\pi m_in_0(V_g^2 - C_s^2)}\right]k_\xi^2V_g'. \tag{4.1}$$

In the following, we study the frequency of the perturbed wave from (4.1) by using the plasma parameters (Kostrov *et al.* 2003) $B_0 = 6.5 \times 10^{-3}$ T, $n_0 = 1.2 \times 10^{18}\,\mathrm{m}^{-3}$,

https://doi.org/10.1017/S002237782400014X Published online by Cambridge University Press

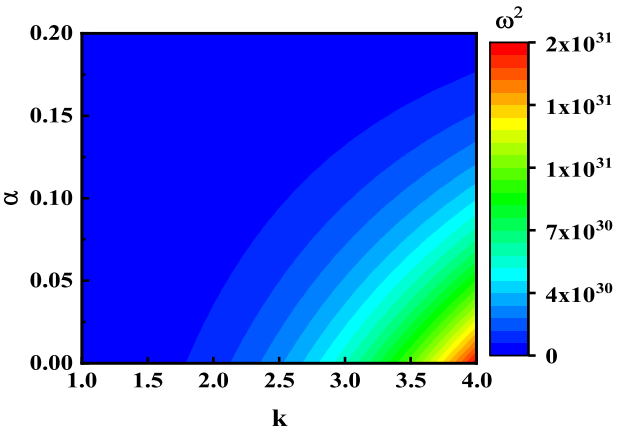

FIGURE 1. Dependence of ω^2 on both perturbed wavenumber k and α with $B_0 = 6.5 \times 10^{-3}$ T, $n_0 = 1.2 \times 10^{18}\,\mathrm{m}^{-3}$, $\omega_{\mathrm{pe}} = 6.7 \times 10^{10}\,\mathrm{s}^{-1}$, $\omega_{\mathrm{ce}} = 1.76 \times 10^{9}\,\mathrm{s}^{-1}$, $T_e = 1.16 \times 10^{5}$ K, $T_i = 5.8 \times 10^{3}$ K, $C_s = 5.25 \times 10^{3}\,\mathrm{m\,s}^{-1}$, $C_A = 2.9 \times 10^{4}\,\mathrm{m\,s}^{-1}$, $m_i/m_e = 73\,400$, $m_e = 9.11 \times 10^{31}$ kg, $a_0 = 1$.

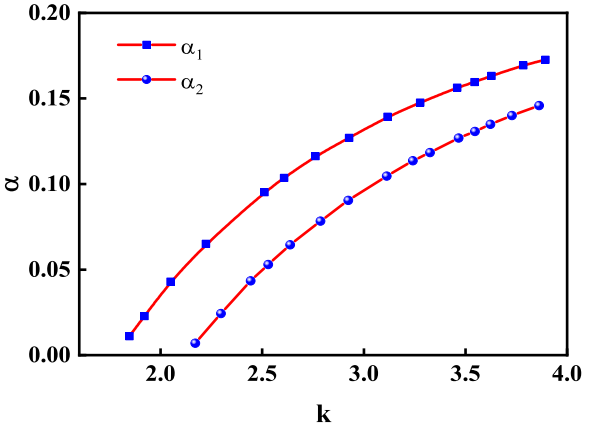

FIGURE 2. Dependence of α on k where $\omega^2 = 7.4\,\mathrm{s}^{-2}$ and $\omega^2 = 1.5\,\mathrm{s}^{-2}$ in two curves, respectively, the other parameters are $B_0 = 6.5 \times 10^{-3}$ T, $n_0 = 1.2 \times 10^{18}\,\mathrm{m}^{-1}$, $\omega_{\mathrm{pe}} = 6.7 \times 10^{10}\,\mathrm{s}^{-1}$, $\omega_{\mathrm{ce}} = 1.76 \times 10^{9}\,\mathrm{s}^{-1}$, $T_e = 1.16 \times 10^{5}$ K, $T_i = 5.8 \times 10^{3}$ K, $C_s = 5.25 \times 10^{3}\,\mathrm{m\,s}^{-1}$, $C_A = 2.9 \times 10^{4}\,\mathrm{m\,s}^{-1}$, $m_i/m_e = 73\,400$, $m_e = 9.11 \times 10^{-31}$ k, $a_0 = 1$.

$\omega_{\mathrm{pe}} = 6.7 \times 10^{10}\,\mathrm{s}^{-1}$, $\omega_{\mathrm{ce}} = 1.76 \times 10^{9}\,\mathrm{s}^{-1}$, $T_e = 1.16 \times 10^{5}$ K, $T_i = 5.8 \times 10^{3}$ K, $C_s = 5.25 \times 10^{3}\,\mathrm{m\,s}^{-1}$, $C_A = 2.9 \times 10^{4}\,\mathrm{m\,s}^{-1}$, $m_i/m_e = 73\,400$, $m_e = 9.11 \times 10^{-31}$ kg, $a_0 = 1$.

Figure 1 shows the dependence of ω^2 on parameters of both k and α. It is observed that the frequency approaches zero as both k and α tend to zero. The frequency increases as k increases. Furthermore, it is zero when $k < 1.78$. However, the frequency decreases as α increases.

In order to further understand the variation of the frequency with respect to both k and α, figure 2 shows the dependence of α on k when ω remains a constant.

https://doi.org/10.1017/S002237782400014X Published online by Cambridge University Press

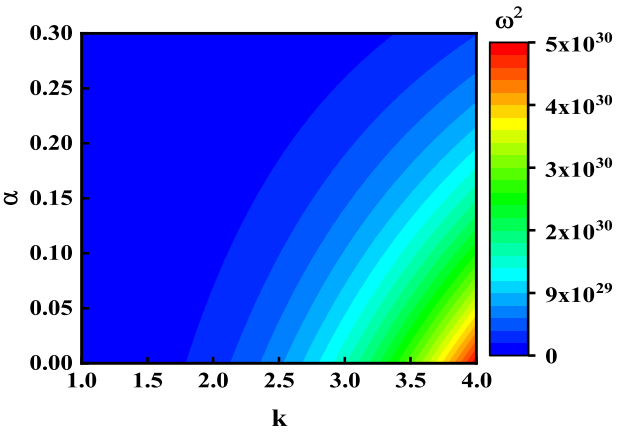

FIGURE 3. Dependence of ω^2 on both perturbed wavenumber k and α with $B_0 = 6.5 \times 10^{-3}$ T, $n_0 = 1.2 \times 10^{18}\,\mathrm{m}^{-3}$, $\omega_{pe} = 6.7 \times 10^{10}\,\mathrm{s}^{-1}$, $\omega_{ce} = 1.76 \times 10^{9}\,\mathrm{s}^{-1}$, $T_e = 1.16 \times 10^{5}$ K, $T_i = 5.8 \times 10^{3}$ K, $C_s = 5.25 \times 10^{3}\,\mathrm{m\,s}^{-1}$, $C_A = 2.9 \times 10^{4}\,\mathrm{m\,s}^{-1}$, $m_i/m_e = 73\,400$, $m_e = 9.11 \times 10^{-31}$ kg, $a_0 = 1$.

The fitted equations of two curves in figure 2 are as follows:

$$\left.\begin{aligned}\alpha_1 &= (-0.92)\exp(-k_1/1.22) + 0.21,\\ \alpha_2 &= (-0.97)\exp(-k_2/1.31) + 0.20.\end{aligned}\right\} \tag{4.2}$$

Second, $(k_x, k_y, k_\xi) = (k_x, 0, 0)$, about which the propagation direction of the perturbed wave is perpendicular to that of the external magnetic field. Then (3.33) becomes

$$\omega^2 = \left[\frac{1}{4}k_x^2 T + \frac{\epsilon\omega_0 a_0^2(1-\alpha)}{8\pi m_i n_0 (V_g^2 - C_s^2)} + \frac{\omega_0 a_0^2 Q\epsilon(\alpha V_g^2 + C_s^2 - 2\alpha C_s^2)}{8\pi m_i n_0 (V_g^2 - C_s^2)}\right] k_x^2 T. \tag{4.3}$$

We also use the same system parameters (Kostrov *et al.* 2003): $B_0 = 6.5 \times 10^{-3}$ T, $n_0 = 1.2 \times 10^{18}\,\mathrm{m}^{-3}$, $\omega_{pe} = 6.7 \times 10^{10}\,\mathrm{s}^{-1}$, $\omega_{ce} = 1.76 \times 10^{9}\,\mathrm{s}^{-1}$, $T_e = 1.16 \times 10^{5}$ K, $T_i = 5.8 \times 10^{3}$ K, $C_s = 5.25 \times 10^{3}\,\mathrm{m\,s}^{-1}$, $C_A = 2.9 \times 10^{4}\,\mathrm{m\,s}^{-1}$, $m_i/m_e = 73\,400$, $m_e = 9.11 \times 10^{-31}$ kg, $a_0 = 1$.

Figure 3 shows the dependence of ω^2 on parameters of both k and α. It is observed that the frequency approaches zero as both k and α tend to zero. The frequency increases as k increases. Furthermore, it is zero when $k < 1.78$. However, the frequency decreases as α increases.

In order to further understand the variation of the frequency with respect to both k and α, figure 4 shows the dependence of α on k when ω remains a constant.

The fitted equations of two curves in figure 4 are as follows:

$$\left.\begin{aligned}\alpha_1 &= (-2.04)\exp(-k_1/1.28) + 0.40,\\ \alpha_2 &= (-2.04)\exp(-k_2/1.34) + 0.39.\end{aligned}\right\} \tag{4.4}$$

Third, $(k_x, k_y, k_\xi) = (k, 0, \sigma k)$, where $\sigma = \tan\theta_{xz}$, and θ_{xz} is the angle between the direction of the external magnetic field and the vector of the wavenumber. It stands for the

https://doi.org/10.1017/S002237782400014X Published online by Cambridge University Press

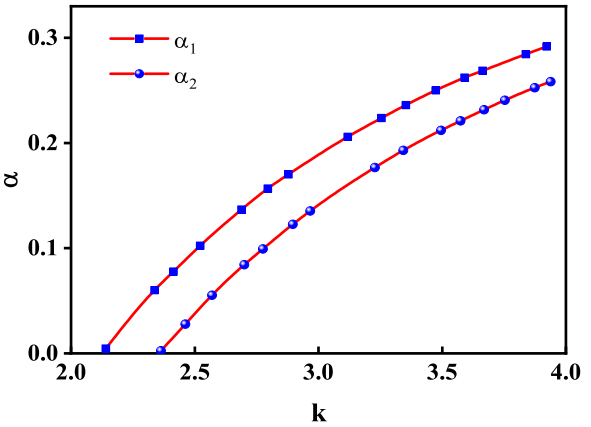

FIGURE 4. Dependence of α on k where $\omega^2 = 3.7\,\mathrm{s}^{-2}$ and $\omega^2 = 5.6\,\mathrm{s}^{-2}$ in two curves, respectively, the other parameters are $B_0 = 6.5 \times 10^{-3}\,\mathrm{T}$, $n_0 = 1.2 \times 10^{18}\,\mathrm{m}^{-3}$, $\omega_{\mathrm{pe}} = 6.7 \times 10^{10}\,\mathrm{s}^{-1}$, $\omega_{\mathrm{ce}} = 1.76 \times 10^{9}\,\mathrm{s}^{-1}$, $T_e = 1.16 \times 10^{5}\,\mathrm{K}$, $T_i = 5.8 \times 10^{3}\,\mathrm{K}$, $C_s = 5.25 \times 10^{3}\,\mathrm{m\,s}^{-1}$, $C_A = 2.9 \times 10^{4}\,\mathrm{m\,s}^{-1}$, $m_i/m_e = 73\,400$, $m_e = 9.11 \times 10^{-31}\,\mathrm{kg}$, $a_0 = 1$.

case in which the perturbed waves propagates in an arbitrary direction, i.e. $0 \leq \theta \leq \pi/2$. For this case, (3.33) becomes

$$\omega^2 = \left[\frac{1}{4}(\sigma^2 k^2 V_g' + k^2 T) + \frac{\epsilon\omega_0 a_0^2(1-\alpha)}{8\pi m_i n_0 (V_g^2 - C_s^2)} - \frac{\omega_0 a_0^2 Q\epsilon(\alpha V_g^2 + C_s^2 - 2\alpha C_s^2)}{8\pi m_i n_0 (V_g^2 - C_s^2)(\sigma^2 - \nu^2)}\right](\sigma^2 k^2 V_g' + k^2 T). \tag{4.5}$$

We also use the same system parameters (Kostrov *et al.* 2003): $B_0 = 6.5 \times 10^{-3}\,\mathrm{T}$, $n_0 = 1.2 \times 10^{18}\,\mathrm{m}^{-3}$, $\omega_{\mathrm{pe}} = 6.7 \times 10^{10}\,\mathrm{s}^{-1}$, $\omega_{\mathrm{ce}} = 1.76 \times 10^{9}\,\mathrm{s}^{-1}$, $T_e = 1.16 \times 10^{5}\,\mathrm{K}$, $T_i = 5.8 \times 10^{3}\,\mathrm{K}$, $C_s = 5.25 \times 10^{3}\,\mathrm{m\,s}^{-1}$, $C_A = 2.9 \times 10^{4}\,\mathrm{m\,s}^{-1}$, $m_i/m_e = 73\,400$, $m_e = 9.11 \times 10^{-31}\,\mathrm{kg}$, $a_0 = 1$, $\sigma = 1$.

Figure 5 shows the dependence of ω^2 on parameters of both k and α. It is observed that the frequency approaches zero as both k and α tend to zero. The frequency increases as k increases. Furthermore, it is zero when $k < 1.78$. However, the frequency decreases as α increases.

In order to further understand the variation of the frequency with respect to both k and α, figure 6 shows the dependence of α on k when ω remains a constant.

The fitted equations of two curves in figure 6 are as follows:

$$\left.\begin{aligned}\alpha_1 &= (-1.23)\exp(-k_1/1.38) + 0.24,\\ \alpha_2 &= (-1.23)\exp(-k_2/1.44) + 0.24.\end{aligned}\right\} \tag{4.6}$$

5. Instability conditions of the perturbed wave

The above study shows that $\omega^2 > 0$, which indicates that there is no instability. However, for different parameters, instability may exist. Figure 7 shows the dependence of ω^2 on the parameters of both σ and k_0, where $\alpha < 1$ since $\omega_0 < \omega_{\mathrm{ce}}$ and $\alpha = \omega_0/\omega_{\mathrm{ce}}$. It is shown in figure 7 that $\omega^2 < 0$ for both the first case and the second case in certain regions, where $k = 0.001$. It seems from figure 7 that ω^2 may be negative in some regions when

https://doi.org/10.1017/S002237782400014X Published online by Cambridge University Press

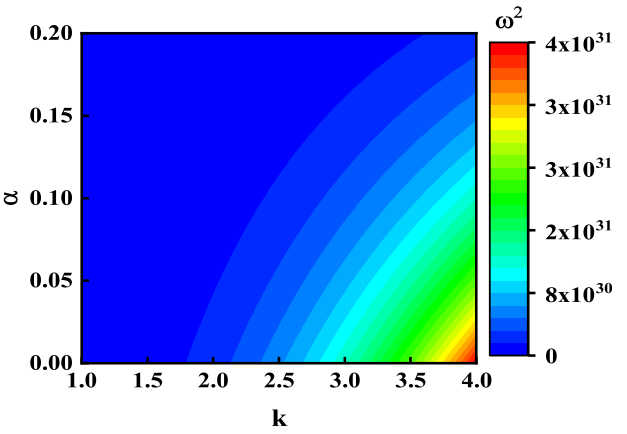

FIGURE 5. Dependence of ω^2 on both perturbed wavenumber k and α with $B_0 = 6.5 \times 10^{-3}$ T, $n_0 = 1.2 \times 10^{18}\,\mathrm{m}^{-3}$, $\omega_{pe} = 6.7 \times 10^{10}\,\mathrm{s}^{-1}$, $\omega_{ce} = 1.76 \times 10^{9}\,\mathrm{s}^{-1}$, $T_e = 1.16 \times 10^{5}$ K, $T_i = 5.8 \times 10^{3}$ K, $C_s = 5.25 \times 10^{3}\,\mathrm{m\,s}^{-1}$, $C_A = 2.9 \times 10^{4}\,\mathrm{m\,s}^{-1}$, $m_i/m_e = 73\,400$, $m_e = 9.11 \times 10^{-31}$ kg, $a_0 = 1$, $\sigma = 1$.

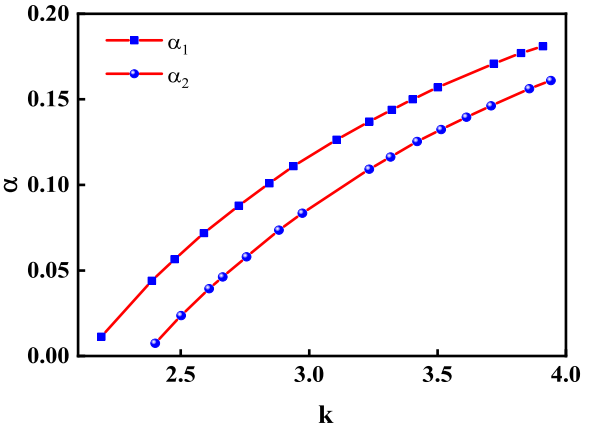

FIGURE 6. Dependence of α on k where $\omega^2 = 3.3\,\mathrm{s}^{-2}$ and $\omega^2 = 5.0\,\mathrm{s}^{-2}$ in two curves, respectively, the other parameters are $B_0 = 6.5 \times 10^{-3}$ T, $n_0 = 1.2 \times 10^{18}\,\mathrm{m}^{-3}$, $\omega_{pe} = 6.7 \times 10^{10}\,\mathrm{s}^{-1}$, $\omega_{ce} = 1.76 \times 10^{9}\,\mathrm{s}^{-1}$, $T_e = 1.16 \times 10^{5}$ K, $T_i = 5.8 \times 10^{3}$ K, $C_s = 5.25 \times 10^{3}\,\mathrm{m\,s}^{-1}$, $C_A = 2.9 \times 10^{4}\,\mathrm{m\,s}^{-1}$, $m_i/m_e = 73\,400$, $m_e = 9.11 \times 10^{-31}$ kg, $a_0 = 1$, $\sigma = 1$.

$k_0 < 0.05$. Furthermore, ω^2 decreases as the σ increases. However, ω^2 increases as the whistler wavenumber k_0 increases. It suggests that there is instability when the whistler wave propagates perpendicular to or parallel to the direction of the external magnetic field. However, it is found that $\omega^2 > 0$ is always satisfied for the third case, which means that it is stable if the angle between the external magnetic field and the perturbed wave's direction is $\pi/4$ ($\sigma = 1$).

Figure 8 shows ω^2 is positive when $k_0 > 0.05$. Here ω^2 increases as the σ increases when $\sigma > 25$. Whereas, ω^2 first increases as k_0 increases, reaches a peak value, and then decreases as k_0 increases.

https://doi.org/10.1017/S002237782400014X Published online by Cambridge University Press

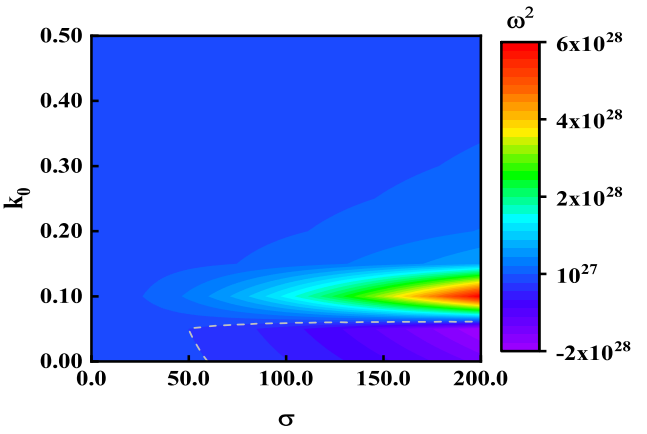

FIGURE 7. Dependence of ω^2 on the wave propagation direction σ and the whistle wave number k_0 where $k = 0.001$, $B_0 = 6.5 \times 10^{-3}$ T, $n_0 = 1.2 \times 10^{18}\,\mathrm{m}^{-3}$, $\omega_{\mathrm{pe}} = 6.7 \times 10^{10}\,\mathrm{s}^{-1}$, $\omega_{\mathrm{ce}} = 1.76 \times 10^{9}\,\mathrm{s}^{-1}$, $T_e = 1.16 \times 10^{5}$ K, $T_i = 5.8 \times 10^{3}$ K, $C_s = 5.25 \times 10^{3}\,\mathrm{m\,s}^{-1}$, $C_A = 2.9 \times 10^{4}\,\mathrm{m\,s}^{-1}$, $m_i/m_e = 73\,400$, $m_e = 9.11 \times 10^{-31}$ kg, $a_0 = 1$, $k_b = 1.38 \times 10^{-23}\,\mathrm{J\,K}^{-1}$, $\epsilon_0 = 8.85 \times 10^{-12}\,\mathrm{F\,m}^{-1}$, $\mu_0 = 1.26 \times 10^{-6}\,\mathrm{H\,m}^{-1}$.

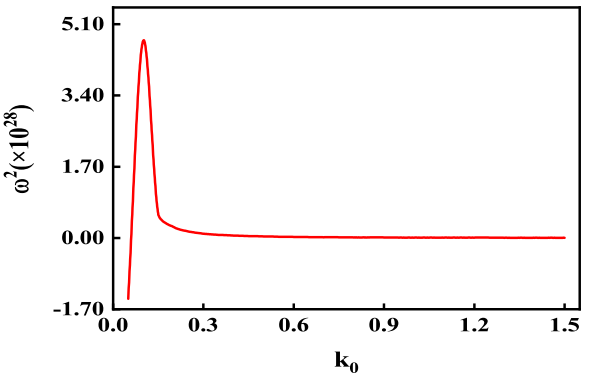

FIGURE 8. Dependence of ω^2 on k_0 where $k = 0.001$, $\sigma = 180$, $k = 0.001$, $B_0 = 6.5 \times 10^{-3}$ T, $n_0 = 1.2 \times 10^{18}\,\mathrm{m}^{-3}$, $\omega_{\mathrm{pe}} = 6.7 \times 10^{10}\,\mathrm{s}^{-1}$, $\omega_{\mathrm{ce}} = 1.76 \times 10^{9}\,\mathrm{s}^{-1}$, $T_e = 1.16 \times 10^{5}$ K, $T_i = 5.8 \times 10^{3}$ K, $C_s = 5.25 \times 10^{3}\,\mathrm{m\,s}^{-1}$, $C_A = 2.9 \times 10^{4}\,\mathrm{m\,s}^{-1}$, $m_i/m_e = 73\,400$, $m_e = 9.11 \times 10^{-31}$ kg, $a_0 = 1$, $k_b = 1.38 \times 10^{-23}\,\mathrm{J\,K}^{-1}$, $\epsilon_0 = 8.85 \times 10^{-12}\,\mathrm{F\,m}^{-1}$, $\mu_0 = 1.26 \times 10^{-6}\,\mathrm{H\,m}^{-1}$.

6. Conclusion

The present investigation focuses on the modulational instability of the nonlinearly interacting electron whistlers and magnetosonic perturbations. It is found that the wave is modulational stable for typical plasma parameters. However, modulational instability appears in special cases. The results show that modulational instability appears in some regions when the whistler wavenumber satisfies $k_0 < 0.05$. Moreover, the growth rate decreases as the angle between the external magnetic field and the perturbed wave's direction increases. However, the growth rate increases as the whistler wavenumber k_0 increases.

It is also found that there is no modulational instability when the whistler wavenumber satisfies $k_0 > 0.05$. In this case, the perturbed wave frequency increases as the angle

https://doi.org/10.1017/S002237782400014X Published online by Cambridge University Press

between the external magnetic field and the perturbed wave's direction increases when the angle between the external magnetic field and the perturbed wave's direction is large enough. Whereas, the perturbed wave frequency first increases as the whistler wavenumber increases, reaches a peak value and then decreases as whistler wavenumber increases.

Acknowledgements

This work was supported by the National Natural Science Foundation of China (NSFC) (nos. 12275223, 11965019, 42004131, 42065005) and by the Foundation of Gansu Educational Committee (no. 2022QB-178).

Editor T. Carter thanks the referees for their advice in evaluating this article.

Declaration of interests

The authors report no conflict of interest.

REFERENCES

BELL, T., INAN, U., BORTNIK, J. & SCUDDER, J. 2002 The landau damping of magnetospherically reflected whistlers within the plasmasphere. *Geophys. Res. Lett*. **29** (15), 1733.

CHOI, S., BESSHO, N., WANG, S., CHEN, L. & HESSE, M. 2022 Whistler waves generated by nongyrotropic and gyrotropic electron beams during asymmetric guide field reconnection. *Phys. Plasmas* **29**, 012903.

DAS, A., SINGH, R., KAW, P. & CHAMPEAUX, S. 2002 Nonlinear coupling of whistler wave turbulence with magnetosonic perturbations. *Phys. Plasmas* **9**, 2609–2618.

ELIASSON, B. & SHUKLA, P. 2005*a* Linear self-focusing of whistlers in plasmas. *New J. Phys*. **7**, 95.

ELIASSON, B. & SHUKLA, P. 2005*b* Three-dimensional dynamics of nonlinear whistlers in plasmas. *Phys. Lett.* A **348**, 51–57.

FUJIMOTO, K. & SYDORA, R. 2008 Whistler waves associated with magnetic reconnection. *Geophys. Res. Lett*. **35**, L19112.

GASTER, M. & GRANT, I. 1975 An experimental investigation of the formation and development of a wave packet in a laminar boundary layer. *Proc. R. Soc. Lond.* A **347**, 253–269.

GUPTA, N., CHOUDHRY, S. & BHARDWAJ, S. 2023 Plasma crystal. *Appl. Spectrosc*. **89** (6), 1168–1176.

GUROVICH, V. & KARPMAN, V. 1969 Dynamics of electroacoustic waves in fluids and plasma. *Sov. Phys. JETP* **29** (6), 1048–1055.

GUSHCHIN, M., KOROBKOV, S., KOSTROV, A. & STRIKOVSKY, A. 2004 Compression of whistler waves in a plasma with a nonstationary magnetic field. *J. Expl Theor. Phys*. **99** (5), 978–986.

GUSHCHIN, M., KOROBKOV, S., KOSTROV, A., STRIKOVSKY, A. & ZABORONKOVA, T. 2005 Propagation of whistlers in a plasma with a magnetic field duct. *JETP Lett*. **81** (5), 214–217.

HORNE, R., THORNE, R., SHPRITS, Y., MEREDITH, N., GLAUERT, S., SMITH, A., KANEKAL, S., BAKER, D., ENGEBRETSON, M., POSCH, J., *et al.* 2005 Wave acceleration of electrons in the van allen radiation belts. *Nature* **437**, 227–230.

HOSHINO, M., MUKAI, T., TERASAWA, T. & SHINOHARARAO, I. 2001 Suprathermal electron acceleration in magnetic reconnection. *J. Geophys. Res*. **106** (A11), 25979–25997.

HUANG, G., WANG, D. & SONG, Q. 2004 Whistler waves in freja observations. *J. Geophys. Res*. **109**, A02307.

INAN, U. 1987 Waves and instabilities. *Rev. Geophys*. **25** (3), 588–598.

KARPMAN, V., KAUFMAN, R. & SHAGALOV, A. 1992 Self-focusing of whistler waves. *Phys. Plasmas* **4**, 3087–3100.

KARPMAN, V., LYNOV, J., MICHELSEN, P. & JUUL, R. 1995 Nonlinear evolution of whistler wave modulational instability. *Phys. Plasmas* **2**, 3302–3319.

KARPMAN, V. & SHAGALOV, A. 1984 Self-focusing and the two-dimensional collapse of whistlers. *Sov. Phys. JETP* **87**, 422–432.

KIVSHAR, Y. 1992 Modnlational instabilities in discrete lattices. *Phys. Rev.* A **46** (6), 3198–3205.

KOSTROV, A., GUSHCHIN, M., KOROBKOV, S. & STRIKOVSKI, A. 2003 Parametric transformation of the amplitude and frequency of a whistler wave in a magnetoactive plasma. *J. Expl Theor. Phys*. **78** (9), 538–541.

LI, S., ZHANG, S., CAI, H., DENG, X. & YANG, H. 2014 Observation and analysis of whistler-mode wave and electrostatic solitary waves within density depletion near magnetic reconnection x-line. *Sci. China Phys. Mech*. **57** (4), 652–658.

LI, X., WANG, R. & LU, Q. 2023 Division of magnetic flux rope via magnetic reconnection observed in the magnetotail. *Geophys. Res. Lett*. **50**, e2022GL101084.

MEIER, J., STEGEMAN, G., CHRISTODOULIDES, D., SILBERBERG, Y., MORANDOTTI, R., YANG, H., SALAMO, G., SOREL, M. & AITCHISON, J. 2004 Experimental observation of discrete modulational instability. *Phys. Rev. Lett*. **92** (16), 163902–1–163902–4.

NASSIRI, M. 2008 Whistler wave propagation in field-aligned density duct plasma. *Europhys. Lett*. **82**, 35001.

SHUKLA, P., MOND, M., KOURAKIS, I. & ELIASSON, B. 2005 Nonlinearly coupled whistlers and dust-acoustic perturbations in dusty plasmas. *Phys. Plasmas* **12**, 124502.

SHUKLA, P. & STENFLO, L. 1995 Nonlinear alfvén waves. *Phys. Scr*. **T60**, 32–35.

SINGH, N. 2013 Propagation and dispersion of whistler waves generated by fast reconnection onset. *Phys. Plasmas* **20**, 022106.

STENZEL, R. 1999 Whistler waves in space and laboratory plasmas. *J. Geophys. Res*. **104** (A7), 14379–14395.

SUTHERLAND, O., GILES, M. & BOSWELL, R. 2005 Ion cyclotron production by a four-wave interaction with a helicon pump. *Phys. Rev. Lett*. **94**, 205002.

TAI, K., HASEGAWA, A. & TOMITA, A. 1986 Observation of modnlational instability in optical fibers. *Phys. Rev. Lett*. **56** (2), 135–139.

TRIPATHI, V. & KUMARA, P. 2008 Parametric conversion of a lower hybrid wave into a whistler in a plasma. *Phys. Plasmas* **15**, 052107.

TSKHAKAYA, D. 1981 On the 'non-stationary' ponderomotive force of a hf field in a plasma. *J. Plasma Phys*. **25**, 233–238.

ZHU, M., LIU, Y., WEI, C., NI, H. & WEI, Q. 2023 Ionization induced by the ponderomotive force in intense and high-frequency laser fields. *J. Chem. Phys*. **158**, 164306.

https://doi.org/10.1017/S002237782400014X Published online by Cambridge University Press